Macromolecules

pubs.acs.org/Macromolecules Article

Living Direct Arylation Polymerization via C−H Activation for the Precision Synthesis of Polythiophenes and Their Block Copolymers

Si-Lin Huang, Chen-Chen Ye, Ya-Nan Pan, Qiao-Yun Liu, Chao Wang, and Lei Xu*

Cite This: *Macromolecules* 2025, 58, 2357−2365 Read Online

ACCESS | Metrics & More | Article Recommendations | Supporting Information

ABSTRACT: P3HT, a typical conjugated polymer, is widely applied in field-effect transistors and photovoltaic devices owing to its excellent properties, relatively low cost, and synthetic versatility. However, existing P3HT synthesis methods suffer from poor atom economy, complicated procedures, and environmental pollution. Herein, we present a living direct arylation polymerization method via C−H bond activation, which eliminates the need for cumbersome Grignard, boron, and stannylated reagents. Polythiophene synthesis is achieved with 90% regioregularity, a narrow molecular weight distribution (M_w/M_n), and controlled molecular weight (M_n) by using an air-stable palladium catalyst via catalyst-transfer polycondensation. The chemical structures of the resulting polythiophenes, which feature the Pd(II) complex at polymer chain ends, were confirmed by nuclear magnetic resonance spectroscopy, matrix-assisted laser desorption/ionization time-of-flight mass spectrometry with end-group analysis, and chain-extension experiments. Furthermore, amphipathic polythiophene block copolymers and polythiophene-*block*-poly(phenyl isocyanide) were synthesized by using the isolated P3HT-Pd(II) as the macroinitiator, and their self-assembly was systematically investigated. The self-assembled amphipathic polythiophene block copolymers demonstrate intriguing fluorescence characteristics and emit white fluorescent light.

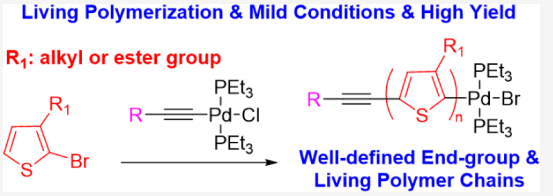

INTRODUCTION

Conjugated polymers, especially polythiophene, are employed in organic electronic devices, including solar cells, light-emitting diodes, memory devices, and sensing technologies.[1−3] However, device performance is closely linked to the conjugated polymer structure, necessitating the development of novel and precise synthesis methods.[4] Chain growth (or living) polymerization plays a central role in polymer chemistry, enabling precise control over molecular weight distribution and polymer design, including the synthesis of block copolymers with well-defined terminal structures.[5−8] Conjugated polymers are commonly synthesized via Kumada, Sonogashira, Suzuki, and Stille cross-coupling polymerization reactions using nickel or palladium catalysts, achieving quasi-living catalyst-transfer polymerization.[3] However, these traditional methods often require halogenated and metallic functional groups and have notable drawbacks. For example, their need for prefunctionalized monomers often involves the use of cumbersome reagents such as Grignard, boron, and stannylated compounds. Additionally, these methods suffer from low atom economy, complex procedures, and environmental pollution, which increase synthesis complexity and costs.[9−16] Recent advancements in direct arylation polymerization (DArP) include single-step activation and arylation of aromatic C−H bonds to simplify and efficiently synthesize conjugated polymers.[17−22] Direct (hetero)arylation polymerization was initially reported by Lemaire et al. in 1999.[23,24] This approach follows a C−H activation pathway, enhancing atom efficiency, reducing synthetic steps, minimizing environmental impact, and producing only harmless byproducts compared to earlier polymerization methods.[25,26] DArP has been extensively researched for over a decade and stands as a promising approach for synthesizing well-defined conjugated polymers.[27−30] Synthesizing high-quality polymers with less toxic reagents and fewer steps than earlier methods makes DArP a viable option for industrial-scale conjugated polymer production.[31,32] However, the high C−H bond energy makes direct polymerization difficult, especially in living polymerization.

The development of living DArP with controlled molecular weight (M_n) and narrow molar mass dispersity (M_w/M_n) distribution holds scientific significance.[9] Polymerization depends on forming a metal−polymer π-complex, allowing the catalyst to migrate to the growing polymer chain end and promoting intramolecular oxidative addition.[10,15] Recently, Luscombe et al. reported the living DArP of P3HT with orthogonal reactivity utilizing dual-metal catalysis.[33,34] However, DArP typically requires high temperature, high pressure, and long polymerization times, resulting in high energy consumption and low reaction control.[35] Developing living

Received: December 5, 2024
Revised: February 19, 2025
Accepted: February 20, 2025
Published: February 27, 2025

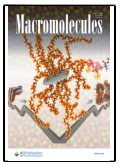

https://doi.org/10.1021/acs.macromol.4c03027
Macromolecules 2025, 58, 2357−2365

Table 1. Optimization of the DArP Condition with 2-Bromo-3-Hexylthiophene (1) Using Palladium Catalysts

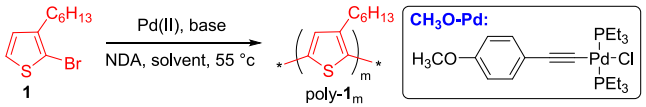

run[a]	Pd	solvent	base	M_n (kDa)[b]	M_w/M_n[b]	Yield[c]
1	$Pd(dppf)Cl_2$	DMA	K_3PO_4	6.93	1.72	90%
2	$Pd(OAc)_2$	DMA	K_3PO_4	12.64	3.13	92%
3	$Pd(PPh_3)_4$	DMA	K_3PO_4	--[d]	--	--
4	$Pd(PPh_3)_2Cl_2$	DMA	K_3PO_4	7.06	1.67	85%
5	$Pd(COD)Cl_2$	DMA	K_3PO_4	8.53	2.89	81%
6	$Pd_2(dba)_3$	DMA	K_3PO_4	7.39	2.47	92%
7	CH_3O–Pd	DMA	K_3PO_4	4.37	1.23	91%
8	CH_3O–Pd	THF	K_3PO_4	--	--	--
9	CH_3O–Pd	Tol.	K_3PO_4	--	--	--
10	CH_3O–Pd	DMF	K_3PO_4	7.52	1.76	45%
11	CH_3O–Pd	$CHCl_3$	K_3PO_4	--	--	--
12	CH_3O–Pd	EA	K_3PO_4	--	--	--
13	CH_3O–Pd	DMA	K_2CO_3	--	--	--
14	CH_3O–Pd	DMA	Cs_2CO_3	3.12	1.48	27%
15	CH_3O–Pd	DMA	Na_2CO_3	--	--	--
16	CH_3O–Pd	DMA	Et_3N	--	--	--
17	CH_3O–Pd	DMA/THF (3/1)	K_3PO_4	4.71	1.10	92%
18	CH_3O–Pd	DMA/THF (3/3)	K_3PO_4	12.24	2.25	90%
19	CH_3O–Pd	DMA/THF/H_2O (3/1/0.1)	K_3PO_4	5.12	1.24	95%

[a]These polymers were synthesized according to Scheme in Table 1. The same polymerization conditions was $[\mathbf{1}]_0$ = 0.1 M, $[\mathbf{1}]_0/[Pd(II)]_0$ = 30, 55 °C, 24 h. [b]The M_n and M_w/M_n values were determined by SEC with reference to polystyrene standards. [c]The isolated yields. [d]Not detected.

DArP under mild conditions while controlling M_w/M_n and M_n is meaningful.[36] By employing an air-stable Pd(II) catalyst during thiophene polymerization, Pd(II) complexes at polymer chain ends can be efficiently recovered, enhancing the ecofriendliness of the process.[7,37−39] Subsequently, these living polymer chains can be end-capped or chain extended to synthesize block copolymers. For example, in the synthesis of poly(3-hexylthiophene)-*block*-poly(phenyl isocyanide) (P3HT-*b*-PPI), initiating the polymerization of isocyanide with a palladium complex at the chain end yields higher stereoregular polyisocyanides, in contrast to P3HT-*b*-PPI synthesized using a nickel complex as the initiator.[7,37,40] Polythiophene block copolymers exhibit remarkable self-assembly and luminescence, making them highly suitable for semiconductor applications.[41,42]

Herein, we describe a novel method for synthesizing polythiophene via living DArP. The initiation reaction proceeds faster than the propagation reaction during polymerization, and the structures of the propagating species remain well-defined owing to the stability of the terminal group. This method enables the efficient precision synthesis of polythiophene with a narrow M_w/M_n distribution and controlled M_n at lower temperatures and faster reaction rates compared to previous polymerization methods. The synthesized polymers were systematically characterized, and the presence of active end groups was confirmed through matrix-assisted laser desorption-ionization time-of-flight mass spectrometry (MALDI-TOF MS), ^{1}H nuclear magnetic resonance spectroscopy (NMR), ^{31}P NMR, and chain-extension reactions. Importantly, our living DArP method enables the synthesis of functional polythiophene with ester substituents, which is impossible via traditional Kumada coupling polymerization. In addition, the synthesis of P3HT block copolymers employing the isolated P3HT-Pd(II) as the macroinitiator via identical (poly($\mathbf{1}_m$-*b*-$\mathbf{4}_n$)) and different (poly($\mathbf{1}_m$-*b*-$\mathbf{5}_n$)) block polymerization mechanisms was explored. Finally, the self-assembly behavior and fluorescence properties of polythiophene block copolymers were investigated.

RESULTS AND DISCUSSION

Monomer **1** was utilized as a model to optimize the polymerization conditions, as listed in Table 1. Determination of the optimal polymerization conditions was contingent upon the selection of a suitable Pd catalyst, solvent, and base. Polymerization reactions of **1** using Pd catalysts were conducted under a nitrogen atmosphere at 55 °C in neodecanoic acid (NDA, 0.3 equiv) for 24 h ($[\mathbf{1}]_0$ = 0.1 M, $[\mathbf{1}]_0/[Pd(II)]_0$ = 30). The post-treatment procedure involved cooling the reaction system to room temperature, adding a large amount of MeOH to remove low-molecular-weight impurities, and centrifuging to obtain the polymer, which was subsequently dried and weighed to determine the yield. First, we conducted a series of experiments using different Pd complexes (runs 1−7, Table 1). Polymerization reactions employing $Pd(dppf)Cl_2$, $Pd(OAc)_2$, $Pd(PPh_3)_4$, $Pd(PPh_3)_2Cl_2$, $Pd(COD)Cl_2$, and $Pd_2(dba)_3$ afforded poly-$\mathbf{1}_m$ with a wide M_w/M_n distribution (Figure S1); however, using CH_3O–Pd(II) as the initiator afforded poly-$\mathbf{1}_m$ with a narrow M_w/M_n distribution and in high yield (run 7, Table 1). Subsequently, we explored different solvents (runs 7−12, Table 1), including *N*,*N*-dimethylacetamide (DMA), tetrahydrofuran (THF), toluene (tol.), *N*,*N*-dimethylformamide (DMF), $CHCl_3$, and ethyl acetate (EA), using CH_3O–Pd(II) as the initiator, discovering that polymerization could be completed in DMA and DMF. DMA was the best solvent, affording polymers with a narrow M_w/M_n distribution (runs 7 and 10, Table 1 and Figure S2). Finally, we explored different bases, such as K_3PO_4, K_2CO_3, Na_2CO_3, and Et_3N (runs 13−16, Table 1), discovering

https://doi.org/10.1021/acs.macromol.4c03027
Macromolecules 2025, 58, 2357−2365

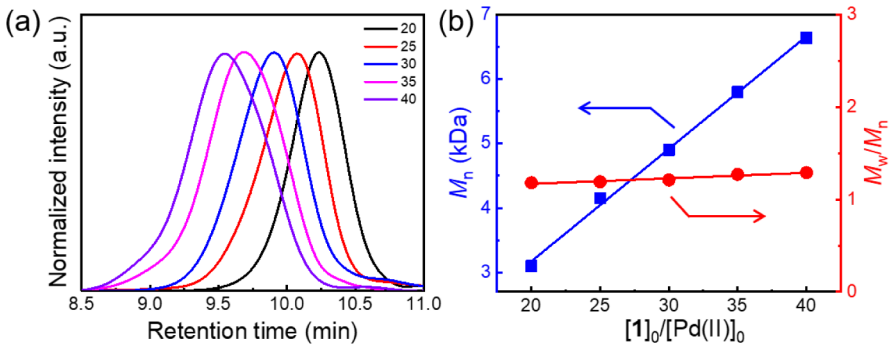

Figure 1. (a) SEC of poly-$\mathbf{1}_m$ prepared with different initial monomer (**1**)-to-catalyst (CH_3O−Pd(II)) feed ratios. (b) Plots of M_n and M_w/M_n values of poly-$\mathbf{1}_m$ with different initial monomer (**1**)-to-catalyst (CH_3O−Pd(II)) feed ratios (SEC conditions: eluent, THF; temperature, 40 °C).

Scheme 1. Chain-Extension Polymerization in One-Pot

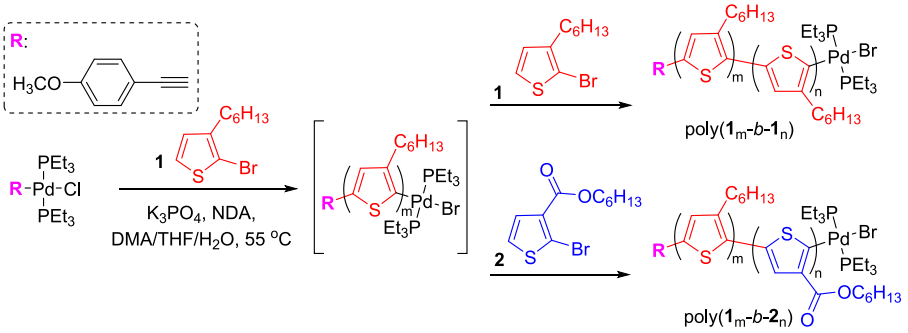

that polymerization could be achieved in K_3PO_4 and Cs_2CO_3. K_3PO_4 was the best base, affording poly-$\mathbf{1}_m$ with a narrow M_w/M_n distribution and desired M_n (Figure S3). Adding THF to the polymerization system facilitated the synthesis of poly-$\mathbf{1}_m$ with a higher M_n (runs 17 and 18, Table 1 and Figure S4) but a wider M_w/M_n distribution. Monomer conversion reached 41% after 12 h, which increased to 94% after 48 h (Figure S5). Furthermore, adding 0.1 mL of H_2O to the DMA/THF (3/1, v/v) system accelerated polymerization, affording polymers with the desired M_n and narrow M_w/M_n distribution (run 19, Table 1). The reaction system transitioned from light yellow to red after 12 h (Figure S6).

The best polymerization conditions were determined to be CH_3O−Pd(II) as the initiator, K_3PO_4 as the base, in DMA/THF/H_2O (3/1/0.1), at 55 °C, and [**1**] = 0.1 M. The isolated poly-$\mathbf{1}_{30}$ (footnote indicating the initial monomer-to-catalyst feed ratio) had an M_n of 5.12 kDa, and a low M_w/M_n value of 1.24, which suggested that polymerization proceeded *via* a living chain growth mechanism. To validate this hypothesis, polymerization reactions of **1** using CH_3O−Pd(II) as the catalyst were conducted in DMA/THF/H_2O (3/1/0.1) at 55 °C under identical experimental conditions but various initial monomer-to-catalyst feed ratios. The polymerization reactions proceeded smoothly with high yields (>85%) of the expected polymers (Table S1). As depicted in Figure 1, the isolated polymers displayed unimodal, symmetrical SEC elution peaks, shifting toward higher M_n with increased monomer (**1**)-to-catalyst (CH_3O−Pd(II)) ratio while maintaining a low M_w/M_n value (<1.29).

To verify the living nature of the chain ends of the resulting poly-$\mathbf{1}_m$-Pd(II), one-pot, two-step chain-extension experiments were performed with **1** using poly-$\mathbf{1}_{25}$-Pd(II) (M_n = 4.08 kDa, M_w/M_n = 1.28) as the macroinitiator (Scheme 1). First, **1** was treated with poly-$\mathbf{1}_{25}$-Pd(II) to verify the living nature of the Pd(II) complex terminus of the poly-$\mathbf{1}_m$ segment ($[\mathbf{1}]_0/[Pd(II)]_0$ = 15). As shown in Figure 2, the elution peak of the

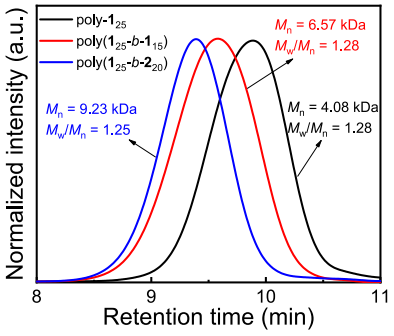

Figure 2. SEC chromatograms of chain-extended polymers: poly-$\mathbf{1}_{25}$, poly($\mathbf{1}_{25}$-*b*-$\mathbf{1}_{15}$), and poly($\mathbf{1}_{25}$-*b*-$\mathbf{2}_{20}$).

resulting chain-extended poly-$\mathbf{1}_{25}$-Pd(II) shifted toward a higher M_n as compared to the poly-$\mathbf{1}_{25}$-Pd(II) precursor. The M_n value of poly-$\mathbf{1}_m$-Pd(II) increased to 6.57 kDa (M_w/M_n = 1.28). To better understand this chain-extension polymerization, one-pot, two-step experiments were performed with monomer **2** using poly-$\mathbf{1}_{25}$-Pd(II) as the macroinitiator ([**2**] = 0.2 M, $[\mathbf{2}]_0/[Pd(II)]_0$ = 20). After 48 h of reaction, the polymerization solution was precipitated by using a large amount of MeOH. The resulting block copolymer, poly($\mathbf{1}_{25}$-*b*-$\mathbf{2}_{20}$), was centrifuged in 80% yield. The M_n value of poly($\mathbf{1}_{25}$-*b*-$\mathbf{2}_{20}$) was estimated to be 9.23 kDa, exhibiting a symmetrical and unimodal elution curve during SEC with a narrow M_w/M_n distribution (Figure 2). Poly($\mathbf{1}_{25}$-*b*-$\mathbf{2}_{20}$) was further characterized by ^{1}H NMR, Fourier-transform infrared spectroscopy (FT-IR), and UV−Vis spectroscopy (Figures S7−S9). The results unequivocally demonstrated the successful occurrence

https://doi.org/10.1021/acs.macromol.4c03027
Macromolecules 2025, 58, 2357−2365

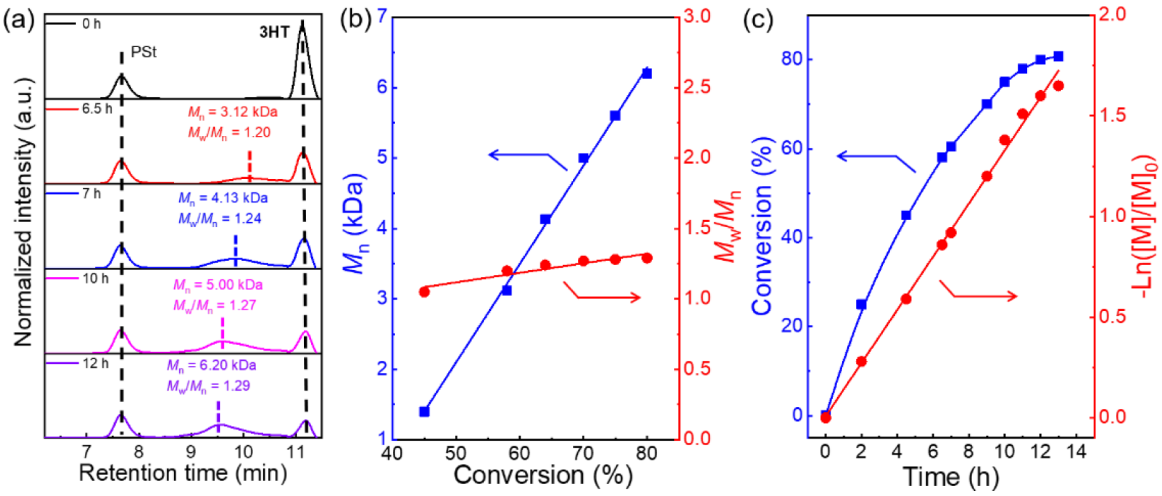

Figure 3. (a) Time-dependent SEC chromatograms of P3HT for the polymerization of monomer **1**, using polystyrene (M_n = 126 kDa, M_w/M_n = 1.04) as the internal standard, initiated by CH_3O−Pd(II) in DMA/THF/H_2O (3/1/0.1, v/v/v) at 55 °C. (b) Plots of M_n and monomer conversion. (c) Plots of conversion and first-order kinetics of monomer **1** with polymerization time.

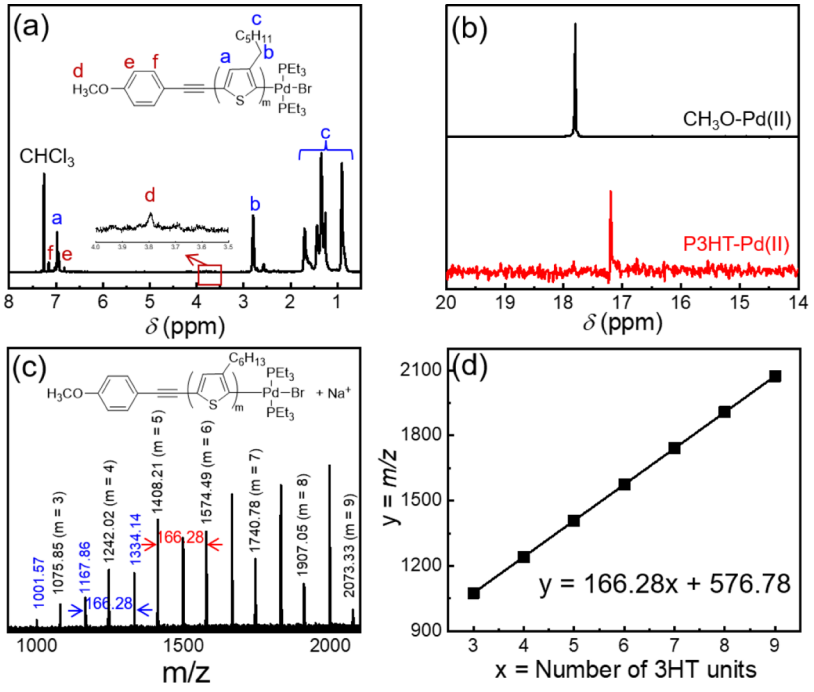

Figure 4. (a) ^{1}H NMR spectrum of poly-**1**$_m$ and (b) ^{31}P NMR spectra of CH_3O−Pd(II) and poly-**1**$_m$. (c) MALDI-TOF MS spectrum of poly-**1**$_m$ produced by living DArP. (d) Plots of m/z versus number of repeating **1** units.

and progression of chain-extension polymerization in a living manner.

To verify the absence of chain transfer and termination reactions during the polymerization process, experiments were conducted to explore whether monomers were exclusively utilized in chain growth reactions. The polymerization of monomer **1** with CH_3O−Pd(II) was conducted in DMA/THF/H_2O (3/1/0.1, v/v/v) at 55 °C, using polystyrene (M_n = 126 kDa, M_w/M_n = 1.04) as an internal standard, and the resulting polymers were characterized by SEC to assess monomer conversion, M_n, and M_w/M_n at various polymerization times (Figure 3a). The monomer concentration gradually decreased, and polymers emerged with increasing polymerization time, accompanied by an increase in M_n owing to monomer transformation. Notably, the M_w/M_n distribution remained consistently narrow throughout the process (Figure 3a,b). Monomer conversion reached 80% after polymerization for 12 h, affording a polymer with an M_n value of 6.20 kDa. Consequently, the entire polymerization process could be regarded as a living chain growth mechanism. Notably, polymerization was revealed to obey first-order reaction kinetics (Figure 3c). The polymer appearance rate constant was estimated to be 3.68 × 10^{-5} s^{-1}, further confirming the living nature of the polymerization process. The monomer conversion rate measured by SEC was only 80% due to the influence of certain low-molecular-weight additives in the reaction system, such as NDA and DMA. To accurately determine the conversion rate of the polymerization system, we employed ^{1}H NMR at different reaction times (Figure S10), revealing 94% conversion after 15 h.

https://doi.org/10.1021/acs.macromol.4c03027
Macromolecules 2025, 58, 2357−2365

Scheme 2. Proposed Plausible Mechanism for the Catalyst Transfer Living DArP

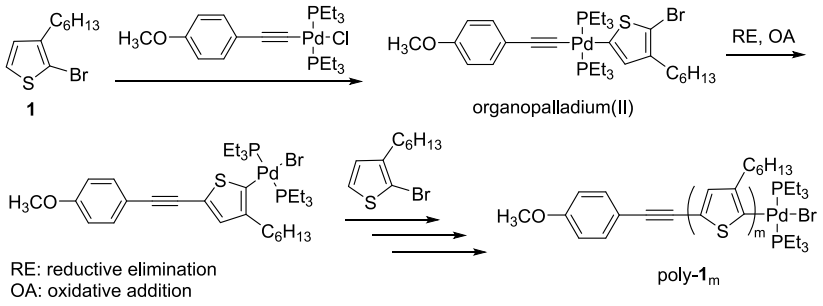

In addition to SEC analysis, the well-defined polymers were characterized by ^{1}H and ^{31}P NMR, MALDI-TOF MS, and FT-IR (Figures 4 and S11). Integrating the α-methylene signals of the 3-hexyl groups at δ 2.81 (HT) and 2.58 (HH) revealed 90% regioregularity (Figure 4a).[43,44] During defect analysis in the aromatic region, the 4-position of the 3-hexylthiophene unit in the HT−HT linkage was observed at δ 6.98, and major signals were assignable to other regioisomers and β-defects.[43,44] Moreover, weak signals attributed to the ArH and CH_3O groups of the terminal unit were observed at δ 7.16 (f), 6.83 (e), and 3.81 (d) ppm, respectively. The ^{31}P NMR spectrum of CH_3O−Pd(II) exhibited a single peak at δ 17.81 ppm (Figure 4b), which vanished upon polymerization of 3HT, accompanied by the emergence of a new broad peak at δ 17.18 ppm, which corresponded to the resulting polymer P3HT. These results suggested that Pd(II) units were located at the terminal groups of the polymers and were stable. Further, we conducted MALDI-TOF MS to determine the chain initiation and termination end groups of P3HT. The obtained mass spectrum exhibited two different types of molecular ions (Figure 4c) that were ascribed to CH_3OPh-P3HT-Pd$(PEt_3)_2$Br ionized by Na^+ and CH_3OPh-P3HT-H ionized by K^+. The relationship between the m/z values of the CH_3OPh-P3HT-Pd$(PEt_3)_2$Br + Na^+ ions in the MS spectrum and the number of repeating 3HT units was expressed as $y = 166.28x + 576.78$, where y is the m/z values of polymer ions and x is the number of 3HT units (Figure 4d). The interval between the two sets of peaks was ∼166.28 g/mol, which aligned with the molecular weight of the 3HT unit. To clearly characterize the terminal groups of the polymers, F−Pd was synthesized as an initiator for the polymerization of 3HT. To accurately ascertain the structure of its end groups, the isolated polymers were characterized by SEC, ^{1}H, ^{19}F, and ^{31}P NMR, and MALDI-TOF MS (Figures S12−S14). The ^{19}F NMR spectrum exhibited a resonance at δ −113.87 ppm, indicative of the presence of end-group fluorobenzene structures (Figure S14a). The ^{31}P NMR spectrum of the isolated P3HT exhibited a resonance similar to the spectrum of P3HT synthesized using CH_3O−Pd(II) as the initiator (Figure S14b). Thus, MALDI-TOF MS analysis indicated the presence of initiating and terminating chain ends (Figure S14c). These results confirmed the formation of polymers with well-defined termination end groups and structures, supporting the generation of active living chain ends.

Thiophene polymers featuring ester functionalities exhibit exceptional properties, rendering them highly versatile for the development of advanced device materials.[45,46] Our established living DArP method offers the benefits of polymerization of thiophene monomers bearing side-chain esters in high yield with controllable M_n and a narrow M_w/M_n distribution (Figures S15−S19).

Most Pd-catalyzed cross-coupling reactions with (hetero)-aryl molecules proceed through a similar catalytic cycle.[6,14] The proposed mechanism for living DArP is outlined in Scheme 2. First, **1** reacts with CH_3O−Pd(II), yielding the organopalladium(II) compound. The organopalladium(II) compound subsequently undergoes reductive elimination and oxidative addition to generate new Pd complexes. To understand the initiation polymerization reaction, stoichiometric reactions were monitored via ^{1}H NMR. The initiation polymerization reaction followed first-order kinetics with a rate constant of 1.18×10^{-3} s^{-1} (Figure S20), indicating that the chain initiation rate was greater than the chain growth rate. Thus, polymer chain growth proceeds via the sequential insertion of monomers, as illustrated in the reaction cycle, with the Pd(II) moiety consistently serving as the polymer chain's end group.

Synthesis of Polythiophene Block Copolymers Using "Living" P3HT-Pd(II) Macroinitiator. To prove that its activity was maintained, isolated poly-$\mathbf{1}_{25}$-Pd(II) was employed as the macroinitiator in the polymerization of monomer **4** for the synthesis of all-conjugated amphiphilic polythiophene diblock copolymers, poly($\mathbf{1}_m$-*b*-$\mathbf{4}_n$), according to Scheme 3.

Scheme 3. Synthesis of Amphiphilic Poly($\mathbf{1}_m$-*b*-$\mathbf{4}_n$) Block Copolymers

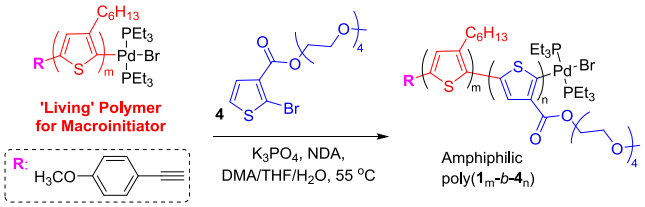

The SEC elution curve of poly($\mathbf{1}_{25}$-*b*-$\mathbf{4}_{10}$) (M_n = 7.42 kDa, M_w/M_n = 1.29) revealed a shorter retention time than that of the macroinitiator P3HT-Pd(II), with a symmetric and unimodal elution peak (Figure 5a). Poly($\mathbf{1}_{25}$-*b*-$\mathbf{4}_{10}$) was characterized by ^{1}H NMR (Figure S21), showing resonances at δ 6.98, 2.80, and 1.70−0.85 ppm for the poly-$\mathbf{1}_m$ segment and at δ 7.90, 4.46, and 3.81−3.35 ppm for the poly-$\mathbf{4}_n$ segment. Further characterization of poly($\mathbf{1}_m$-*b*-$\mathbf{4}_n$) was performed by using FT-IR (Figure S22).

Moreover, the all-conjugated amphiphilic polythiophene diblock copolymers possessed the ability to crystallize and self-assemble in selective solvents.[47] Poly($\mathbf{1}_{25}$-*b*-$\mathbf{4}_{10}$) was dissolved in toluene, a solvent compatible with both blocks. Aggregation was triggered by adding MeOH, which selectively solvated the

https://doi.org/10.1021/acs.macromol.4c03027
Macromolecules 2025, 58, 2357−2365

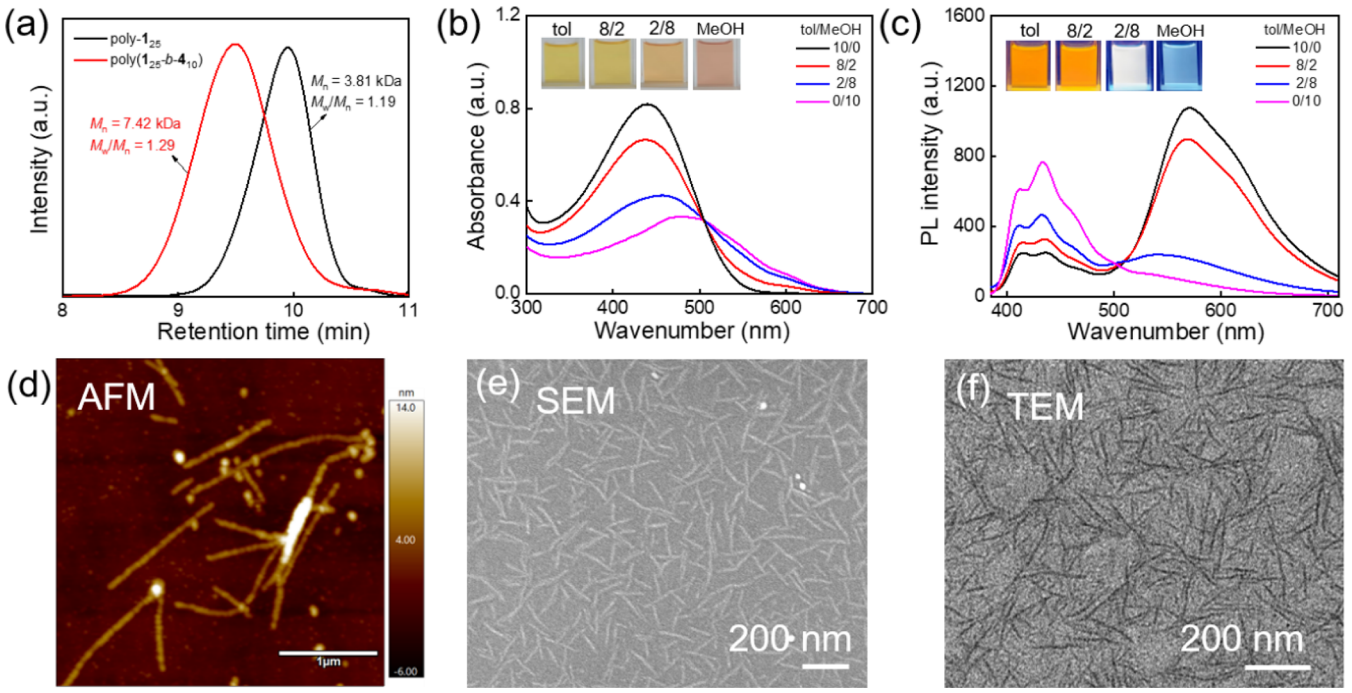

Figure 5. (a) SEC chromatograms of the P3HT-Pd(II) macroinitiator and poly($\mathbf{1}_{25}$-*b*-$\mathbf{4}_{10}$) block copolymer. (b) UV−vis and (c) emission spectra of poly($\mathbf{1}_{25}$-*b*-$\mathbf{4}_{10}$) in tol./MeOH (c = 0.2 mg/mL, λ_{exc} = 365 nm). (d) AFM, (e) SEM, and (f) TEM images of poly($\mathbf{1}_{25}$-*b*-$\mathbf{4}_{10}$) in tol./MeOH (8/2, v/v, c = 0.2 mg/mL).

poly-$\mathbf{4}_n$ block. The UV−Vis absorption spectra of poly($\mathbf{1}_{25}$-*b*-$\mathbf{4}_{10}$) in tol./MeOH are presented in Figure 5b. Poly($\mathbf{1}_{25}$-*b*-$\mathbf{4}_{10}$) in tol. exhibited a substantial absorption band in the longer wavelength region with a maximum absorption peak at 439 nm, which was attributed to polythiophenes. Upon adding MeOH, this peak intensity decreased, accompanied by a red shift, while two new peaks emerged at 546 and 602 nm, indicating $\pi-\pi$ stacking and crystalline aggregation of the P3HT block (Figure 5b). The photoluminescence spectrum of poly($\mathbf{1}_{25}$-*b*-$\mathbf{4}_{10}$) in tol./MeOH (Figure 5c) revealed that the emission intensity in the 495−700 nm region gradually decreased with increasing MeOH content, whereas that in the 384−495 nm region increased. These emission changes were attributed to the solvophobic effect of amphiphilic poly($\mathbf{1}_{25}$-*b*-$\mathbf{4}_{10}$), which induced self-assembly and led to the formation of distinct supramolecular architectures. The block copolymers self-assembled into nanofiber structures in toluene/MeOH (8/2, v/v), as evidenced by the atomic force microscopy (AFM) image shown in Figure 5d, with approximate diameters and heights of 150 and 8 nm, respectively. Formation of these supramolecular structures was further confirmed by scanning electron microscopy (SEM) (Figure 5e) and transmission electron microscopy (TEM) (Figure 5f). The results supported the successful synthesis of all-conjugated amphiphilic polythiophene diblock copolymers by using the isolated macroinitiator. We investigated the effect of temperature on the morphology of block copolymers poly($\mathbf{1}_{25}$-*b*-$\mathbf{4}_{10}$) in tol./MeOH (8/2, v/v). The morphology was characterized by SEM (Figure S23a,b). SEM images revealed that at 40 °C, the copolymers formed both spherical and fibrous nanoparticles, whereas at 50 °C, all nanoparticles were spherical with an average diameter of approximately 40 nm. The decrease in particle size with increasing temperature was attributed to the thermoresponsiveness of the amphiphilic polymer, which enhances aggregation at higher temperatures. Emission spectra and fluorescence photograph measurements at different temperatures showed slight variations (Figure S23c).

Phenyl isocyanides readily polymerize using a Pd(II) complex as the initiator.[4,10,37] Thus, the isolated living P3HT-Pd(II) was utilized as a macroinitiator for the polymerization of monomer **5** in toluene at 90 °C with varying initial monomer **5** to macroinitiator P3HT-Pd(II) feed ratios, aiming to synthesize P3HT-*b*-PPI block copolymers according to Scheme 4 ([**5**]$_0$ = 0.2 M, [**5**]$_0$/[P3HT-Pd(II)]$_0$ =

Scheme 4. Synthesis of P3HT-*b*-PPI Block Copolymers

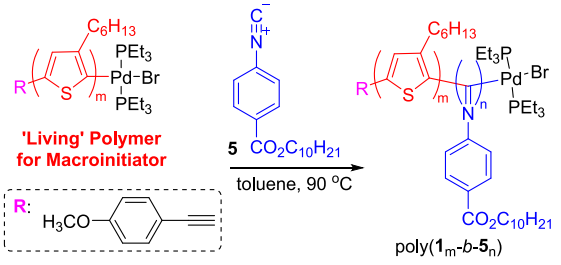

10−100). We also attempted the polymerization of monomer **5** in THF at 55 °C; however, the reaction proceeded slowly, yielding less than 60% polymer after 12 h, with a significant amount of unreacted monomer. Insertion of the PPI block occurred through a polymerization mechanism that differed from that of the P3HT block. After 12 h of reaction, the polymerization solution was precipitated in excess MeOH, and the solid was collected by centrifugation, affording block copolymers in high yields. Successful polymerization was determined by SEC. As shown in Figure 6a, the resulting polymers exhibited symmetric and unimodal elution peaks. The SEC chromatograms of the resulting block copolymers

https://doi.org/10.1021/acs.macromol.4c03027
Macromolecules 2025, 58, 2357−2365

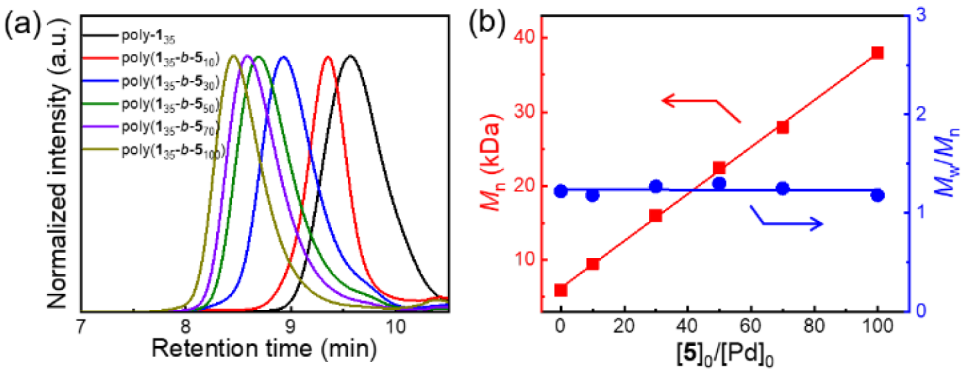

Figure 6. (a) SEC of poly($\mathbf{1}_{35}$-*b*-$\mathbf{5}_n$) block copolymers with different ratios of monomer to P3HT-Pd(II) macroinitiator. (b) Plot of M_n and M_w/M_n values of poly($\mathbf{1}_{35}$-*b*-$\mathbf{5}_n$) block copolymers.

exhibited shorter retention times than that of the macroinitiator P3HT-Pd(II). Plots of the M_n and M_w/M_n values of the block copolymers with various initial monomer **5** to macroinitiator P3HT-Pd(II) feed ratios are presented in Figure 6b. M_n of the block copolymers increased linearly and proportionately with the initial monomer **5** to macroinitiator P3HT-Pd(II) feed ratio, demonstrating a narrow M_w/M_n distribution. These results indicated that the isolated living P3HT could initiate the polymerization of isocyanide monomers in a living chain growth manner. In addition to SEC analysis, the chemical structures of the resulting block polymers were verified by ^{1}H NMR and FT-IR (Figures S24 and S25). The ^{1}H NMR spectrum of poly($\mathbf{1}_m$-*b*-$\mathbf{5}_n$) copolymer displayed resonances at δ 6.98 and 2.80 ppm, corresponding to the aryl and CH_2 protons of the P3HT segment, respectively. Additionally, signals at δ 7.45−7.04 and 5.95−5.34 ppm were attributed to the aryl protons of the PPI segment, while the resonance at δ 4.21−3.56 ppm was assigned to the CO_2CH_2 proton of the PPI block. The FT-IR spectrum of poly($\mathbf{1}_m$-*b*-$\mathbf{5}_n$) exhibited characteristic peaks at 1604 and 1720 cm^{-1}, corresponding to the C═N group of the PPI main chain and ester groups of the side chains, respectively (Figure S25). Photographs of poly($\mathbf{1}_{35}$-*b*-$\mathbf{5}_{30}$) in tol./MeOH mixture at different volume ratios, captured under room light and under UV-365 nm, are shown in Figure S26. Due to the solvophobic and $\pi-\pi$ interaction of the P3HT block, the emission color shifted from yellow to red. Additionally, P3HT-*b*-PPI block copolymers were successfully synthesized *via* a one-pot process through the sequential addition of monomer **1** and monomer **5**. The formation of poly-$\mathbf{1}_m$-Pd(II) and P3HT-*b*-PPI was confirmed by SEC (Figure S27), while the structure of P3HT-*b*-PPI was further verified by ^{1}H NMR (Figure S28).

CONCLUSIONS

Herein, we describe a novel living DArP method that enables polythiophene synthesis with controlled M_n, a narrow M_w/M_n distribution, and well-defined end groups. Interestingly, the isolated polymer chains continue to possess activity at their chain ends and are involved in identical and different block polymerization mechanisms. The controlled self-assembly of block copolymers was systematically investigated. The amphipathic polythiophene block copolymers demonstrate intriguing fluorescence characteristics and emit white fluorescent light during different self-assembly states. The present study expands the scope of catalyst-transfer polycondensation during living polymerization and introduces a remarkably simple, mild, atom-economical, and ecofriendly approach for generating high-quality polymers with potential applications in diverse fields, including semiconducting, biomedicine, and optoelectronics.

ASSOCIATED CONTENT

Supporting Information

The Supporting Information is available free of charge at https://pubs.acs.org/doi/10.1021/acs.macromol.4c03027.

Synthetic procedure and additional spectroscopy data (PDF)

AUTHOR INFORMATION

Corresponding Author

Lei Xu − *Key Laboratory of Green and Precise Synthetic Chemistry and Applications, Ministry of Education; Anhui Provincial Key Laboratory of Synthetic Chemistry and Applications; College of Chemistry and Materials Science, Huaibei Normal University, Huaibei, Anhui 235000, PR China;* orcid.org/0000-0002-3290-7526; Email: xulei@chnu.edu.cn

Authors

Si-Lin Huang − *Key Laboratory of Green and Precise Synthetic Chemistry and Applications, Ministry of Education; Anhui Provincial Key Laboratory of Synthetic Chemistry and Applications; College of Chemistry and Materials Science, Huaibei Normal University, Huaibei, Anhui 235000, PR China*

Chen-Chen Ye − *Key Laboratory of Green and Precise Synthetic Chemistry and Applications, Ministry of Education; Anhui Provincial Key Laboratory of Synthetic Chemistry and Applications; College of Chemistry and Materials Science, Huaibei Normal University, Huaibei, Anhui 235000, PR China*

Ya-Nan Pan − *Key Laboratory of Green and Precise Synthetic Chemistry and Applications, Ministry of Education; Anhui Provincial Key Laboratory of Synthetic Chemistry and Applications; College of Chemistry and Materials Science, Huaibei Normal University, Huaibei, Anhui 235000, PR China*

Qiao-Yun Liu − *Key Laboratory of Green and Precise Synthetic Chemistry and Applications, Ministry of Education; Anhui Provincial Key Laboratory of Synthetic Chemistry and Applications; College of Chemistry and Materials Science, Huaibei Normal University, Huaibei, Anhui 235000, PR China*

https://doi.org/10.1021/acs.macromol.4c03027
Macromolecules 2025, 58, 2357−2365

Chao Wang − *Key Laboratory of Green and Precise Synthetic Chemistry and Applications, Ministry of Education; Anhui Provincial Key Laboratory of Synthetic Chemistry and Applications; College of Chemistry and Materials Science, Huaibei Normal University, Huaibei, Anhui 235000, PR China*

Complete contact information is available at: https://pubs.acs.org/10.1021/acs.macromol.4c03027

Notes

The authors declare no competing financial interest.

■ ACKNOWLEDGMENTS

This work is supported by the National Natural Science Foundation of China (NSFC, No. 52303007), the Scientific Research Foundation for Doctoral Studies at Huaibei Normal University (No. 03106219), and the Excellent Youth Research Project of the Anhui Provincial Education Department (No. 2022AH030059).

■ REFERENCES

(1) Freudenberg, J.; Jänsch, D.; Hinkel, F.; Bunz, U. H. F. Immobilization Strategies for Organic Semiconducting Conjugated Polymers. *Chem. Rev.* **2018**, *118* (11), 5598−5689.
(2) Dimov, I. B.; Moser, M.; Malliaras, G. G.; McCulloch, I. Semiconducting Polymers for Neural Applications. *Chem. Rev.* **2022**, *122* (4), 4356−4396.
(3) Ding, L.; Yu, Z.-D.; Wang, X.-Y.; Yao, Z.-F.; Lu, Y.; Yang, C.-Y.; Wang, J.-Y.; Pei, J. Polymer Semiconductors: Synthesis, Processing, and Applications. *Chem. Rev.* **2023**, *123* (12), 7421−7497.
(4) Liu, N.; Gao, R.-T.; Wu, Z.-Q. Helix-Induced Asymmetric Self-Assembly of π-Conjugated Block Copolymers: From Controlled Syntheses to Distinct Properties. *Acc. Chem. Res.* **2023**, *56* (21), 2954−2967.
(5) Wakioka, M.; Morita, H.; Ichihara, N.; Saito, M.; Osaka, I.; Ozawa, F. Mixed-Ligand Approach to Palladium-Catalyzed Direct Arylation Polymerization: Synthesis of Donor-Acceptor Polymers Containing Unsubstituted Bithiophene Units. *Macromolecules* **2020**, *53* (1), 158−164.
(6) Cheng, S.; Zhao, R.; Seferos, D. S. Precision Synthesis of Conjugated Polymers Using the Kumada Methodology. *Acc. Chem. Res.* **2021**, *54* (22), 4203−4214.
(7) Liu, N.; Zhou, L.; Wu, Z.-Q. Alkyne-Palladium(II)-Catalyzed Living Polymerization of Isocyanides: An Exploration of Diverse Structures and Functions. *Acc. Chem. Res.* **2021**, *54* (20), 3953−3967.
(8) Nitto, R.; Ohta, Y.; Yokozawa, T. Suzuki-Miyaura Catalyst-Transfer Condensation Polymerization for the Synthesis of Polyphenylene with Ester Side Chain by Using Stable, Reactive 1,1,2,2-Tetraethylethylene Glycol Boronate (B(Epin)) Monomer. *Macromolecules* **2024**, *57* (3), 985−990.
(9) Pouliot, J.-R.; Grenier, F.; Blaskovits, J. T.; Beaupré, S.; Leclerc, M. Direct (Hetero)arylation Polymerization: Simplicity for Conjugated Polymer Synthesis. *Chem. Rev.* **2016**, *116* (22), 14225−14274.
(10) Su, M.; Liu, N.; Wang, Q.; Wang, H.; Yin, J.; Wu, Z.-Q. Facile Synthesis of Poly(phenyleneethynylene)-*block*-Polyisocyanide Copolymers via Two Mechanistically Distinct, Sequential Living Polymerizations Using a Single Catalyst. *Macromolecules* **2016**, *49* (1), 110−119.
(11) Aplan, M. P.; Gomez, E. D. Recent Developments in Chain-Growth Polymerizations of Conjugated Polymers. *Ind. Eng. Chem. Res.* **2017**, *56* (28), 7888−7901.
(12) Ma, B.; Shi, Q.; Ma, X.; Li, Y.; Chen, H.; Wen, K.; Zhao, R.; Zhang, F.; Lin, Y.; Wang, Z.; et al. Defect-Free Alternating Conjugated Polymers Enabled by Room-Temperature Stille Polymerization. *Angew. Chem., Int. Ed.* **2022**, *61* (16), No. e202115969.
(13) Kleybolte, M. E.; Vagin, S. I.; Rieger, B. High-Molecular-Weight Bisalkoxy-Substituted Poly(para)phenylenes by Kumada Polymerization. *Macromolecules* **2022**, *55* (13), 5361−5370.
(14) Ye, L.; Thompson, B. C. Improving the Efficiency andSustainability of Catalysts for Direct Arylation Polymerization (DArP). *J. Polym. Sci.* **2022**, *60* (3), 393−428.
(15) Lee, J.; Ryu, H.; Park, S.; Cho, M.; Choi, T.-L. Living Suzuki-Miyaura Catalyst-Transfer Polymerization for Precision Synthesis of Length-Controlled Armchair Graphene Nanoribbons and Their Block Copolymers. *J. Am. Chem. Soc.* **2023**, *145* (28), 15488−15495.
(16) Kleine, A.; Kimmig, J.; Mankel, C.; Schubert, U. S.; Jäger, M. Low-Pressure Preparative Size-Exclusion Chromatography: From Narrow Disperse Polymer to Monodisperse Oligomer Batches. *Macromolecules* **2024**, *57* (13), 6090−6099.
(17) Mercier, L. G.; Leclerc, M. Direct (Hetero)Arylation: A New Tool for Polymer Chemists. *Acc. Chem. Res.* **2013**, *46* (7), 1597−1605.
(18) Pankow, R. M.; Thompson, B. C. Approaches for improving the sustainability of conjugated polymer synthesis using direct arylation polymerization (DArp). *Polym. Chem.* **2020**, *11* (3), 630−640.
(19) Kempe, F.; Riehle, F.; Komber, H.; Matsidik, R.; Walter, M.; Sommer, M. Semifluorinated, kinked polyarylenes via direct arylation polycondensation. *Polym. Chem.* **2020**, *11* (43), 6928−6934.
(20) Zhao, B.; Liang, Z.; Zhang, Y.; Sui, Y.; Shi, Y.; Zhang, X.; Li, M.; Deng, Y.; Geng, Y. Direct Arylation Polycondensation toward Water/Alcohol-Soluble Conjugated Polymers: Influence of Side Chain Functional Groups. *ACS Macro Lett.* **2021**, *10* (4), 419−425.
(21) Mayhugh, A. L.; Yadav, P.; Luscombe, C. K. Circular Discovery in Small Molecule and Conjugated Polymer Synthetic Methodology. *J. Am. Chem. Soc.* **2022**, *144* (14), 6123−6135.
(22) Hsu, N. S. Y.; Lin, A.; Uva, A.; Huang, S. H.; Tran, H. Direct Arylation Polymerization of Degradable Imine-Based Conjugated Polymers. *Macromolecules* **2023**, *56* (21), 8947−8955.
(23) Sévignon, M.; Papillon, J.; Schulz, E.; Lemaire, M. New synthetic method for the polymerization of alkylthiophenes. *Tetrahedron Lett.* **1999**, *40* (32), 5873−5876.
(24) Bura, T.; Blaskovits, J. T.; Leclerc, M. Direct (Hetero)arylation Polymerization: Trends and Perspectives. *J. Am. Chem. Soc.* **2016**, *138* (32), 10056−10071.
(25) Chakraborty, B.; Luscombe, C. K. Cross-Dehydrogenative Coupling Polymerization via C−H Activation for the Synthesis of Conjugated Polymers. *Angew. Chem., Int. Ed.* **2023**, *62* (21), No. e202301247.
(26) Wakioka, M.; Ozawa, F. Highly Efficient Catalysts for Direct Arylation Polymerization (DArP). *Asian J. Org. Chem.* **2018**, *7* (7), 1206−1216.
(27) Collier, G. S.; Reynolds, J. R. Exploring the Utility of Buchwald Ligands for C-H Oxidative Direct Arylation Polymerizations. *ACS Macro Lett.* **2019**, *8* (8), 931−936.
(28) Wang, Y.; Hasegawa, T.; Matsumoto, H.; Michinobu, T. Significant Difference in Semiconducting Properties of Isomeric All-Acceptor Polymers Synthesized via Direct Arylation Polycondensation. *Angew. Chem., Int. Ed.* **2019**, *58* (34), 11893−11902.
(29) Pankow, R. M.; Ye, L.; Thompson, B. C. Influence of the Ester Directing Group on the Inhibition of Defect Formation in Polythiophenes with Direct Arylation Polymerization (DArP). *Macromolecules* **2020**, *53* (9), 3315−3324.
(30) Xing, L.; Liu, J.-R.; Hong, X.; Houk, K. N.; Luscombe, C. K. An Exception to the Carothers Equation Caused by the Accelerated Chain Extension in a Pd/Ag Cocatalyzed Cross Dehydrogenative Coupling Polymerization. *J. Am. Chem. Soc.* **2022**, *144* (5), 2311−2322.
(31) Grenier, F.; Aïch, B. R.; Lai, Y.-Y.; Guérette, M.; Holmes, A. B.; Tao, Y.; Wong, W. W. H.; Leclerc, M. Electroactive and Photoactive Poly[Isoindigo-alt-EDOT] Synthesized Using Direct (Hetero)-Arylation Polymerization in Batch and in Continuous Flow. *Chem. Mater.* **2015**, *27* (6), 2137−2143.
(32) Dudnik, A. S.; Aldrich, T. J.; Eastham, N. D.; Chang, R. P. H.; Facchetti, A.; Marks, T. J. Tin-Free Direct C-H Arylation Polymer-

ization for High Photovoltaic Efficiency Conjugated Copolymers. *J. Am. Chem. Soc.* **2016**, *138* (48), 15699−15709.
(33) Suraru, S.-L.; Lee, J. A.; Luscombe, C. K. Preparation of an Aurylated Alkylthiophene Monomer via C−H Activation for Use in Pd-PEPPSI-iPr Catalyzed-Controlled Chain Growth Polymerization. *ACS Macro Lett.* **2016**, *5* (4), 533−536.
(34) Lee, J. A.; Luscombe, C. K. Dual-Catalytic Ag-Pd System for Direct Arylation Polymerization to Synthesize Poly(3-hexylthiophene). *ACS Macro Lett.* **2018**, *7* (7), 767−771.
(35) Ye, L.; Hooshmand, T.; Thompson, B. C. Recycling Heterogenous Catalysts for Multi-Batch Conjugated Polymer Synthesis via Direct Arylation Polymerization. *ACS Macro Lett.* **2022**, *11* (1), 78−83.
(36) Castillo, G. E.; Thompson, B. C. Room Temperature Synthesis of a Well-Defined Conjugated Polymer Using Direct Arylation Polymerization (DArP). *ACS Macro Lett.* **2023**, *12* (10), 1339−1344.
(37) Xue, Y.-X.; Zhu, Y.-Y.; Gao, L.-M.; He, X.-Y.; Liu, N.; Zhang, W.-Y.; Yin, J.; Ding, Y.; Zhou, H.; Wu, Z.-Q. Air-Stable (Phenylbuta-1,3-diynyl)palladium(II) Complexes: Highly Active Initiators for Living Polymerization of Isocyanides. *J. Am. Chem. Soc.* **2014**, *136* (12), 4706−4713.
(38) Ye, S.; Cheng, S.; Pollit, A. A.; Forbes, M. W.; Seferos, D. S. Isolation of Living Conjugated Polymer Chains. *J. Am. Chem. Soc.* **2020**, *142* (25), 11244−11251.
(39) Zhou, L.; Xu, X.-H.; Jiang, Z.-Q.; Xu, L.; Chu, B.-F.; Liu, N.; Wu, Z.-Q. Selective Synthesis of Single-Handed Helical Polymers from Achiral Monomer and a Mechanism Study on Helix-Sense-Selective Polymerization. *Angew. Chem., Int. Ed.* **2021**, *60* (2), 806−812.
(40) Xu, L.; Wang, C.; Li, Y.-X.; Xu, X.-H.; Zhou, L.; Liu, N.; Wu, Z.-Q. Crystallization-Driven Asymmetric Helical Assembly of Conjugated Block Copolymers and the Aggregation Induced White-light Emission and Circularly Polarized Luminescence. *Angew. Chem., Int. Ed.* **2020**, *59* (38), 16675−16682.
(41) Yu, Z.-P.; Liu, N.; Yang, L.; Jiang, Z.-Q.; Wu, Z.-Q. One-Pot Synthesis, Stimuli Responsiveness, and White-Light Emissions of Sequence-Defined ABC Triblock Copolymers Containing Polythiophene, Polyallene, and Poly(phenyl isocyanide) Blocks. *Macromolecules* **2017**, *50* (8), 3204−3214.
(42) Zhang, Y.; Yang, L.; Sun, Y.; Lin, G.; Manners, I.; Qiu, H. Surface-initiated living self-assembly of polythiophene-based conjugated block copolymer into erect micellar brushes. *Angew. Chem., Int. Ed.* **2024**, *63* (9), No. e202315740.
(43) Wang, Q.; Takita, R.; Kikuzaki, Y.; Ozawa, F. Palladium-Catalyzed Dehydrohalogenative Polycondensation of 2-Bromo-3-hexylthiophene: An Efficient Approach to Head-to-Tail Poly(3-hexylthiophene). *J. Am. Chem. Soc.* **2010**, *132* (33), 11420−11421.
(44) Tsuchiya, K.; Ogino, K. Catalytic oxidative polymerization of thiophene derivatives. *Polym. J.* **2013**, *45*, 281−286.
(45) Gobalasingham, N. S.; Noh, S.; Thompson, B. C. Palladium-catalyzed oxidative direct arylation polymerization (Oxi-DArP) of an ester-functionalized thiophene. *Polym. Chem.* **2016**, *7* (8), 1623−1631.
(46) Son, S. Y.; Samson, S.; Siddika, S.; O'Connor, B. T.; You, W. Thermocleavage of Partial Side Chains in Polythiophenes Offers Appreciable Photovoltaic Efficiency and Significant Morphological Stability. *Chem. Mater.* **2021**, *33* (12), 4745−4756.
(47) Lee, E.; Hammer, B.; Kim, J.-K.; Page, Z.; Emrick, T.; Hayward, R. C. Hierarchical Helical Assembly of Conjugated Poly(3-hexylthiophene)-*block*-poly(3-triethylene glycol thiophene) Diblock Copolymers. *J. Am. Chem. Soc.* **2011**, *133* (27), 10390−10393.

https://doi.org/10.1021/acs.macromol.4c03027
Macromolecules 2025, 58, 2357−2365